JHEP|Reports

Liver fibrosis progression analyzed with AI predicts renal decline

Authors

Dan-Qin Sun, Jia-Qi Shen, Xiao-Fei Tong, …, Arun J. Sanyal, Hong You, Ming-Hua Zheng

Correspondence

zhengmh@wmu.edu.cn (M.-H. Zheng), youhongliver@ccmu.edu.cn (H. You).

Graphical abstract

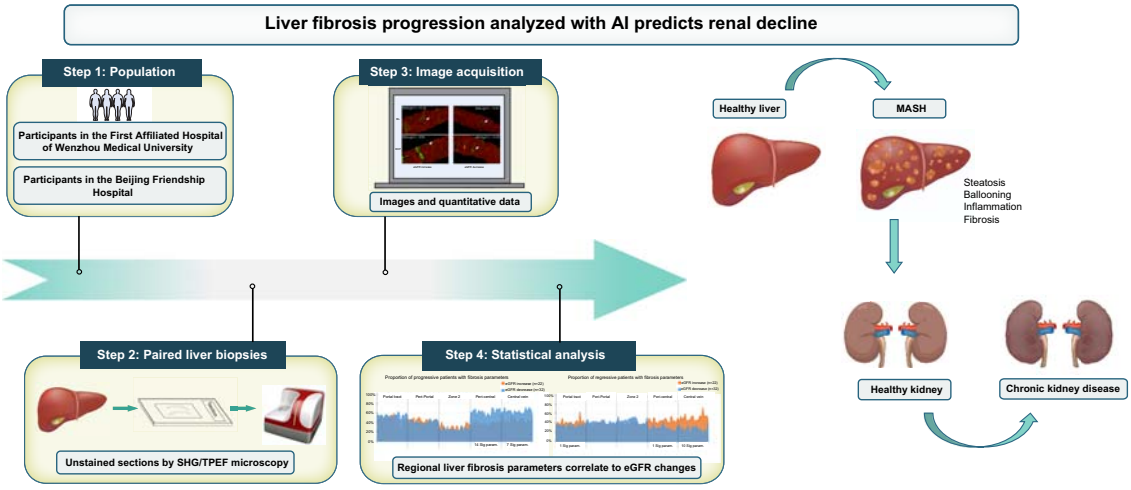

Highlights:

- A decline in renal function is significantly related to liver fibrosis progression in MASLD.
- Liver fibrosis progression in the central vein and pericentral region are strongly related to eGFR decline.
- Predictive models constructed with the qFibrosis parameters could better identify the eGFR decline.

Impact and implications:

The study shows that liver fibrosis progression assessed by qFibrosis may be associated with renal function decline, which provides a new perspective for understanding complex pathological processes. A combination of artificial intelligence and digital pathology may earlier and more precisely quantify the progression of regional liver fibrosis, thus better identifying changes in renal function. This opens the possibility of early interventions, which are essential to improve patients' outcomes.

https://doi.org/10.1016/j.jhepr.2025.101358

JHEP|Reports

Liver fibrosis progression analyzed with AI predicts renal decline

Dan-Qin Sun[1,2,3,†], **Jia-Qi Shen**[1,2,3,†], **Xiao-Fei Tong**[4,†], Ya-Yun Ren[5], Hai-Yang Yuan[6,7,8], Yang-Yang Li[9], Xin-Lei Wang[5], Sui-Dan Chen[9], Pei-Wu Zhu[6], Xiao-Dong Wang[7], Christopher D. Byrne[10], Giovanni Targher[11,12], Lai Wei[13], Vincent W.S. Wong[14], Dean Tai[5], Arun J. Sanyal[15], Hong You[4,*], Ming-Hua Zheng[6,7,8,*]

JHEP Reports **2025**. vol. 7 | 1–12

Background & Aims: The relationship between biopsy-proven liver fibrosis progression and renal function decline in patients with metabolic dysfunction-associated steatotic liver disease (MASLD) has not been fully elucidated. We used an automated quantitative liver fibrosis assessment (qFibrosis) technique to investigate the temporal changes in regional liver fibrosis.

Methods: This retrospective longitudinal study included 68 MASLD patients and their paired formalin-fixed sections of liver biopsies. One hundred eighty-four fibrosis parameters were quantified in five different hepatic regions, including portal tract, periportal, zone 2, peri-central and central vein regions, and qFibrosis continuous values were calculated for all samples based on 10 fibrosis parameters using qFibrosis assessment. Liver fibrosis progression (QLF^+, n = 18) and regression (QLF^-, n = 23) was defined as at least a 20% relative change in qFibrosis over a 23-month follow-up. Renal function decline was assessed by estimated glomerular filtration rate (eGFR) changes.

Results: The eGFR decline was greater in the QLF^+ group (106.53 ± 13.71 ml/min/1.73 m^2 *vs.* 105.28 ± 12.46 ml/min/1.73 m^2) than in the QLF^- group (110.87 ± 14.58 ml/min/1.73 m^2 *vs.* 114.18 ± 14.81 ml/min/1.73 m^2). In addition, liver fibrosis changes in the central vein and pericentral regions were more strongly associated with eGFR decline than in periportal, zone 2 and portal tract regions. We combined these parameters to construct a prediction model, which better differentiated eGFR decline (a cut-off value of qFibrosis combined index = 0.52, p <0.001).

Conclusions: A decline in renal function is significantly related to liver fibrosis progression in MASLD. Regional qFibrosis assessment may efficiently predict eGFR decline, thus highlighting the importance of assessing renal function in patients with MASLD with worsening liver fibrosis.

Introduction

Metabolic dysfunction-associated steatotic liver disease (MASLD), also known as metabolic dysfunction-associated fatty liver disease (MAFLD), affects more than one-third of the world's adult population.[1,2] A significant proportion of these patients will develop metabolic dysfunction-associated steatohepatitis (MASH) with liver injury, inflammation, and varying levels of liver fibrosis.[3] Studies have demonstrated that MASLD is part of a multisystem disease and people with MASLD have not only a higher risk of developing adverse liver-related outcomes, but also important extrahepatic complications, such as cardiovascular disease (CVD), chronic kidney disease (CKD) and certain types of extrahepatic cancers.[4] Notably, the severity of liver fibrosis is the strongest prognostic factor in MASLD and is closely associated with long-term liver-related outcomes and mortality.[5] Consequently, early detection and assessment of liver fibrosis is clinically important.

Liver biopsy has long been the gold standard for fibrosis assessment in MASLD.[6] Despite its capability to provide valuable histopathological information, conventional histological staging of fibrosis is semiquantitative and highly subject to sampling error and observer variations.[7] In recent years, qFibrosis, which is an automated application based on the combination of second harmonic generation/two-photon excitation fluorescence (SHG/TPEF) microscopy with artificial intelligence (AI) analysis,[7,8] has been developed and used for liver fibrosis assessment in MASLD. Wang *et al.*[9] first established an SHG-based quantification of fibrosis-related parameters (Q-FPs) model in patients with MASLD that offered an accurate, reproducible method to assess liver fibrosis along a quantitative and continuous scale. Subsequently, Liu *et al.*[10] showed

* Corresponding authors. Addresses: MAFLD Research Center, Department of Hepatology, the First Affiliated Hospital of Wenzhou Medical University; No. 2 Fuxue Lane, Wenzhou 325000, China, Tel.: +86-577-55579611; fax: +86-577-55578522 (M-H. Zheng); Liver Research Center, Beijing Friendship Hospital, Beijing Key Laboratory of Translational Medicine on Liver Cirrhosis, National Clinical Research Center of Digestive Diseases, Capital Medical University, Beijing 100050, China, Tel.: +86-10-63139019 (H. You).
E-mail addresses: zhengmh@wmu.edu.cn (M.-H. Zheng), youhongliver@ccmu.edu.cn (H. You).
† These authors contributed equally to this work.
https://doi.org/10.1016/j.jhepr.2025.101358

that SHG may reveal subtle fibrosis similarities and differences in adult and pediatric MASLD.[10] Therefore, qFibrosis can effectively overcome some intrinsic limitations of conventional biopsy-based histological fibrosis assessment.

Kidney disease poses a considerable burden on global health as a cause of worldwide morbidity and mortality. In particular, up to nearly 10% of the global adult population has CKD, which results in about 1.2 million deaths and 28 million years of life lost each year.[11] Consequently, timely identification of new and additional risk factors for CKD is particularly valuable in improving long-term clinical outcomes.[12] Convincing clinical evidence[13,14] (including our previously published studies[15,16]) shows that MASLD is strongly associated with an increased long-term risk of CKD, and this CKD risk is further increased with more advanced liver disease, especially with higher fibrosis stage. However, to our knowledge, the evidence for an association between kidney function decline and liver fibrosis progression in people with MASLD, as confirmed by follow-up studies with paired liver biopsies, is limited. Therefore, in this exploratory prospective study, we aimed: (i) to investigate the relationship between temporal changes in liver fibrosis and decline in estimated glomerular filtration rate (eGFR) among patients with MASLD, both at baseline and at follow-up; (ii) to examine whether the use of the qFibrosis tool may better identify subtle liver fibrosis changes (compared with conventional histological liver assessment) and facilitate study of their relationship with eGFR decline; and to (iii) investigate whether regional liver fibrosis parameters could differentiate and predict eGFR decline as a result of liver fibrosis progression in patients with biopsy-confirmed MASLD.

Materials and methods

Study design and population

This retrospective analysis was based on prospectively gathered data. Eligible adult patients (>18 years old) diagnosed with MASLD who underwent two paired liver biopsies from two medical centers in China (the First Affiliated Hospital of Wenzhou Medical University and the Beijing Friendship Hospital) between October 2013 and March 2022, were considered for inclusion. Patients were excluded if they: (1) had a history of significant alcohol consumption (>10 g per day for women and >20 g per day for men); (2) were diagnosed with other chronic liver diseases, such as autoimmune liver disease, viral hepatitis, or secondary fatty liver diseases; (3) developed drug-induced fatty liver disease; (4) used potentially hepatoprotective or hepatotoxic agents; (5) were pregnant or lactating women; (6) had hepatocellular carcinoma or other benign or malignant tumors; (7) had other known causes of chronic or acute kidney diseases as well as presence of urinary tract infection; (8) participated in clinical intervention trials; and (9) had missing data on important clinical or laboratory parameters. Ethical approval for the study was obtained from the ethics committees of each participating center with the project code 2016 No. 246, and written informed consent was obtained from all study participants.

Clinical and laboratory data

Clinical and laboratory parameters were collected in all participants, including age, sex, height, weight, waist circumference, presence of hypertension and diabetes, as well as measurement of serum creatinine, urea nitrogen, low-density lipoprotein cholesterol (LDL-C), high-density lipoprotein cholesterol (HDL-C), serum alanine aminotransferase (ALT) and aspartate aminotransferase (AST) concentrations. As the mean difference in the annual percentage change in eGFR decline in patients with MASLD compared with those without MASLD was approximately -1%,[17] in this study we stratified changes in eGFR levels by at least a 2% relative difference to define the eGFR decrease group (n = 32) and the eGFR increase group (n = 22). In addition, the eGFR levels at the end of follow-up were age- and sex-adjusted in both eGFR patient groups.

Liver biopsy examination

All participants underwent an ultrasound-guided percutaneous liver biopsy. Two independent liver pathologists evaluated the biopsies and scored them according to the MASLD activity score system for liver lesions, including hepatic steatosis, ballooning, lobular inflammation, and fibrosis. MASLD was defined as a grade of 5% or more steatosis with no other competing causes of fatty liver. The histologic features of MASLD were scored according to the non-alcoholic steatohepatitis Clinical Research Network (NASH CRN) classification.[18] The histologic stage of hepatic fibrosis was quantified according to Brunt's criteria.[19] The probability of advanced liver fibrosis was also estimated using two widely used non-invasive scores (NITs) of advanced fibrosis, such as non-alcoholic fatty liver disease (NAFLD) fibrosis score (NFS) and Fibrosis-4 index (FIB-4) scores. The lower cut-off and the upper cut-off for NFS were -1.455 and 0.676, and for FIB-4 index were 1.3 and 2.67, respectively.

SHG/TPEF microscopy and qFibrosis assessment

Unstained sections from participants' paired liver biopsies were examined using SHG/TPEF microscopy with AI analyses. The Genesis®200 (HistoIndex Pte. Ltd, Singapore), a fully automated, stain-free multiphoton fluorescence imaging microscope, was applied to scan the liver sections. Then, the SHG/TPEF images were analyzed using AI-based algorithms. The Genesis®200 utilizes the optical properties of the tissue itself to directly scan an image, which uniquely and sensitively displays collagen changes in the tissue. The same image acquisition parameters were consistently applied to all samples across the two participating centers. The samples were laser excited at 780 nm, SHG signals were recorded at 390 nm, and TPEF signals were recorded at 550 nm. Image tiles were obtained at 20 × magnification, featuring a resolution of 512 × 512 pixels and a dimension of 200 × 200 μm^2. Multiple adjacent image tiles were captured to encompass the entire organizational area on each slide.

The qFibrosis tool is the overall result of assessing liver fibrosis that includes the quantitative results of 184 fibrosis parameters on a linear scale. qFibrosis quantifies overall fibrosis as well as fibrous deposition in five different liver regions (portal tract [PT], periportal [PP], zone 2, pericentral [PC], and central vein [CV] regions), and specific morphological features of collagen fibers, such as fiber length, width, and area. The PP and PC regions are 100 μm from the PT and CV, respectively, and the region between marks zone 2. This measurement of 100 μm approximates one-tenth of the average distance between the PT and CV in a normal liver.

qFibrosis continuous (qFC) values and qFibrosis stages (qFS) were generated for all samples as previously described.[8] The association between liver fibrosis and renal function changes was further investigated by differentiating the increase or decrease in eGFR based on changes in fibrosis parameters in different liver regions. In this study, liver fibrosis progression and regression were defined by the following three methods: (1) a change of at least 1 point in the NASH CRN fibrosis staging was used to classify the fibrosis progression (LF^+, n = 13) and regression (LF^-, n = 28) groups; (2) a change of at least 1 point in the qFibrosis staging was used to classify the fibrosis progression (qLF^+, n = 13) and regression (qLF^-, n = 26) groups; and (3) a relative change of at least 20% in the qFibrosis continuous values or fibrosis parameters was used to classify the fibrosis progression (QLF^+, n = 18) and regression (QLF^-, n = 23) groups during the follow-up period. The NASH CRN fibrosis staging was used to classify no fibrosis change (LF^n, n = 27), the qFibrosis staging was used to classify no fibrosis change (qLF^n, n = 29), and qFibrosis continuous values were used to determine no fibrosis change (QLF^n, n = 27).

We used a sequential feature selection method to select a subset of fibrosis parameters for building a qFibrosis combined index, which may predict the decrease in eGFR at baseline. In the procedure of sequential feature selection, a linear regression model was used, the criterion was the residual sum of squares, and the search algorithm was sequential forward selection. Five fibrosis parameters at baseline, including (1) the percentage of distributed collagen in the tissue, (2) the number of long collagen fibers in the tissue, (3) the number of thin and aggregated collagen fibers in the PP region, (4) the number of long and distributed collagen fibers in CV region, and (5) the number of thin and aggregated collagen fibers for the chicken wire fibrosis, were selected for building the qFibrosis combined index using the linear regression method. Using the Youden's index method, a cut-off value of the combined index could be determined. This suggests that the eGFR will decrease at end of follow-up (EOF) if patients had a combined index larger than the cut-off value at baseline.

Statistical analysis

Statistical analyses were performed using SPSS version 27.0 (IBM; Armonk, NY, USA). Normally distributed continuous variables were expressed as means ± standard deviation (SD), and non-normally distributed ones were expressed as medians (P25, P75). Categorical variables were expressed as counts or percentages (%). The clinical and biochemical characteristics of the study participants were compared using a paired-sample *t* test for continuous variables. The X^2 test was used to estimate the statistical differences in the percentage of regressive/progressive patients between the eGFR increase and decrease groups. The two-tailed Wilcoxon rank-sum test was used to estimate the statistical differences in eGFR changes between the liver fibrosis regression and progression groups. The Spearman's rank correlation analysis assessed the correlation between quantified fibrosis parameters and eGFR values for all participants. The percentages of patients who were regressive/progressive were calculated for eGFR increase and decrease in patients based on the quantified liver fibrosis parameters. The leave-out cross-validation method was used for the model validation cohort of the qFibrosis. Finally, the area under the receiver operating characteristic curve (AUROC) analysis was performed to evaluate the accuracy of the qFibrosis combined index for predicting the changes in eGFR over time. The statistical significance level was set as $p < 0.05$.

Results

Clinical characteristics of biopsy-proven MASLD participants before and after follow-up

A total of 68 middle-aged patients with biopsy-confirmed MASLD were enrolled, including 136 slides of liver tissues. As shown in Table 1, 65% of these patients were male, with a median age of 41 years (range 31–50.8 years), median BMI of 26.6 (23.9, 29.2) kg/m^2, mean waist circumference of 93.00 ± 8.87 cm, and 19%, 24%, and 28% had obesity, diabetes, and hypertension, respectively. Among these patients, the proportion of NFS ≥0.676 and FIB-4 ≥2.67 was 26% and 12%, respectively. Compared with the first liver biopsy examination (baseline), patients at the second liver biopsy examination (follow-up) had lower median MASLD activity scores for hepatic steatosis (2.00 [1.00, 2.75] *vs.* 1.00 [1.00, 2.00]), inflammation (2.00 [1.00, 2.00] *vs.* 1.00 [1.00, 1.00]) and fibrosis (1.00 [1.00, 2.00] *vs.* 1.00 [1.00, 1.00]). The proportion of patients with severe fibrosis (pathology score of 2 or higher) decreased from 43% (29/68) at baseline to 24% (16/68) at follow-up. These patients had significantly lower serum direct bilirubin (DBil), albumin, ALT, AST, and γ-glutamyl-transferase levels, whereas in contrast, higher levels of total bilirubin (TBil), indirect bilirubin (IBil), AST/ALT ratio, blood urea nitrogen (BUN), and HDL-C were observed ($p < 0.05$) at follow-up.

Paired liver specimens from MASLD participants were scanned with Genesis®200 (HistoIndex Pte. Ltd, Singapore) and analyzed quantitatively with qFibrosis, based on which we subdivided the paired liver samples into the QLF^+ (n = 18) and QLF^- (n = 23) groups. The changes from baseline to EOF in clinical and biochemical characteristics of these patient groups are shown in Table 2. In the QLF^- group, those with MASLD had lower histologic fibrosis scores, lower qFS, and lower qFC after EOF than at baseline; the opposite was seen in the QLF^+ group. Also, in either the QLF^+ or QLF^- group, patients with MASLD had lower serum aminotransferase levels than those at baseline ($p < 0.05$), consistent with previous data in Table 1. The QLF^+ group had higher levels of TBil and NFS and lower fasting glucose levels, while the QLF^- group had higher HDL-C and lower DBil after EOF ($p < 0.05$). In the QLF^+ group, the eGFR values slightly decreased in the EOF and QLF^- groups, while the eGFR values increased in the EOF group. Furthermore, we used a multifactor binary logistic regression analysis to investigate the association between changes in QLF and eGFR (Table S1). The results showed that QLF decrease is independently associated with eGFR changes even after adjustment of common renal risk factors, which suggested that QLF decrease may be a protective factor for eGFR increase.

qFibrosis accurately identified the association between liver fibrosis progression and eGFR decline

To better assess the association between liver fibrosis progression and renal function decline, we classified patients with MASLD into fibrosis progression or regression groups based on three different methods, that is, NASH CRN staging,

Table 1. Clinical and biochemical characteristics of patients with MASLD with paired liver biopsies.

Characteristics	First biopsy (n = 68)	Second biopsy (n = 68)	*p* value
Demographics			
Age (years)	41.00 (31.00, 50.75)	42.50 (33.25, 53.00)	<0.001
Male sex (%)	44 (64.71)	44 (64.71)	1.000
BMI (kg/m^2)	26.61 (23.88, 29.20)	24.98 (23.52, 27.68)	<0.001
Diabetes, n (%)	16 (23.53%)	23 (33.82%)	0.184
Hypertension, n (%)	19 (27.94%)	19 (27.94%)	1.000
Angiotensin II receptor blocker, n (%)	5 (7.35%)	5 (7.35%)	1.000
Obesity, n (%)	13 (19.12%)	14 (20.59%)	0.830
Waist circumference (cm)	93.00 ± 8.87	89.72 ± 10.32	<0.001
Laboratory parameters			
WBC (× 10^{12}/L)	6.00 (5.24, 7.09)	5.99 (5.42, 7.11)	0.349
RBC (× 10^{12}/L)	4.91 ± 0.62	4.88 ± 0.63	0.565
Hb (g/L)	147.53 ± 15.26	147.21 ± 16.34	0.811
Platelet count (10^9/L)	239.00 (184.25, 268.25)	216.00 (174.25, 256.00)	<0.001
TBil (μmol/L)	13.00 (11.00, 17.75)	16.50 (12.00, 29.50)	<0.001
DBil (μmol/L)	4.50 (3.00, 6.00)	4.00 (3.00, 6.00)	0.049
IBil (μmol/L)	9.00 (7.00, 12.00)	11.00 (9.00, 14.50)	<0.001
Total cholesterol (mmol/L)	4.97 ± 1.09	4.85 ± 1.08	0.347
Triglycerides (mmol/L)	2.10 (1.53, 2.80)	1.82 (1.43, 2.70)	0.585
Albumin (g/L)	45.23 ± 4.93	44.03 ± 3.75	0.028
ALT (U/L)	70.00 (46.25, 112.25)	32.50 (20.00, 61.75)	<0.001
AST (U/L)	46.00 (34.00, 75.75)	29.00 (19.93, 43.68)	<0.001
AST/ALT ratio	0.61 (0.51,0.91)	0.89 (0.66, 1.15)	<0.001
γ-Glutamyltransferase (U/L)	63.30 (49.00, 88.00)	39.00 (25.00, 58.00)	<0.001
BUN (mmol/L)	4.60 (3.83, 5.50)	5.30 (4.30, 6.30)	0.005
Scr (μmol/L)	66.45 ± 15.13	67.06 ± 17.39	0.598
UA (μmol/L)	381.50 (323.50, 479.50)	368.00 (316.00, 414.00)	0.041
eGFR (ml/min/1.73 m^2)	109.31 ± 13.73	107.41 ± 14.21	0.098
HDL-C (mmol/L)	0.96 (0.87, 1.10)	1.06 (0.92, 1.18)	<0.001
LDL-C (mmol/L)	3.07 ± 0.89	2.92 ± 0.83	0.138
Glucose (mmol/L)	5.35 (4.93, 7.58)	5.50 (4.90, 6.68)	0.366
HOMA-IR score	5.15 (3.25, 8.03)	3.76 (2.52, 7.10)	0.083
NFS	0.00 ± 1.56	0.36 ± 1.62	<0.001
NFS category, n (%)			0.749
NFS <-1.455	8 (11.76)	7 (10.29)	
-1.455≤ NFS <0.676	42 (61.76)	39 (57.35)	
NFS ≥0.676	18 (26.47)	22 (32.35)	
FIB-4 index	1.49 ± 1.37	1.48 ± 1.73	0.982
FIB-4 category, n (%)			0.541
FIB-4 <1.3	45 (66.18)	49 (72.06)	
1.3 ≤ FIB-4 <2.67	15 (22.06)	10 (14.71)	
FIB-4 ≥2.67	8 (11.76)	9 (13.24)	
CKD stage, n (%)			0.345
eGFR ≥90 (ml/min/1.73 m^2)	61 (89.71)	64 (94.12)	
60≤ eGFR <90 (ml/min/1.73 m^2)	7 (10.29)	4 (5.88)	
Liver biopsy			
Steatosis score	2.00 (1.00, 2.75)	1.00 (1.00, 2.00)	<0.001
Severe steatosis (%)	46 (67.65)	23 (33.82)	<0.001
Ballooning score	2.00 (1.00, 2.00)	1.00 (1.00, 2.00)	0.186
Severe ballooning (%)	36 (52.94)	33 (48.53)	0.607
Inflammation score	2.00 (1.00, 2.00)	1.00 (1.00, 1.00)	<0.001
Severe inflammation (%)	36 (52.94)	16 (23.53)	<0.001
Fibrosis score	1.00 (1.00, 2.00)	1.00 (1.00, 1.00)	0.012
Severe fibrosis (%)	29 (42.65)	16 (23.53)	0.018
Steatosis grade			<0.001
0 (%)	0 (0)	9 (13.24)	
1 (%)	22 (32.35)	36 (52.94)	
2 (%)	29 (42.65)	20 (29.41)	
3 (%)	17 (25)	3 (4.41)	
Ballooning grade			0.091
0 (%)	1 (1.47)	7 (10.29)	
1 (%)	31 (45.59)	28 (41.18)	
2 (%)	36 (52.94)	33 (48.53)	
Inflammation grade			0.004
0 (%)	2 (2.94)	7 (10.29)	
1 (%)	30 (44.12)	45 (66.18)	

(*continued on next page*)

Table 1. (*continued*)

Characteristics	First biopsy (n = 68)	Second biopsy (n = 68)	*p* value
2 (%)	33 (48.53)	15 (22.06)	
3 (%)	3 (4.41)	1 (1.47)	
Fibrosis grade			0.086
0 (%)	9 (13.24)	15 (22.06)	
1 (%)	30 (44.12)	37 (54.42)	
2 (%)	16 (23.53)	5 (7.35)	
3 (%)	8 (11.76)	7 (10.29)	
4 (%)	5 (7.35)	4 (5.88)	
qFibrosis stage (qFS)	2.00 (0.00, 2.00)	1.00 (0.00, 2.00)	0.103
qFibrosis continuous value (qFC)	1.17 (0.90, 1.71)	1.07 (0.89, 1.32)	0.188

Data are expressed as means ± SD, medians (P25, P75), or proportions. The paired-sample *t* test was used for comparing normally distributed continuous variables, the Wilcoxon signed-rank test for non-normally distributed variables, and the X^2 test for categorical data.
ALT, alanine aminotransferase; AST, aspartate aminotransferase; BL, baseline; BMI, body mass index; DBil, direct bilirubin; eGFR, estimated glomerular filtration rate; EOF, end of follow up; FIB-4, fibrosis-4 score; Hb, hemoglobin; HDL-C, high-density lipoprotein cholesterol; HOMA-IR, homeostatic model assessment of insulin resistance; IBil, indirect bilirubin; LDL-C, low-density lipoprotein cholesterol; NFS, non-alcoholic fatty liver disease fibrosis score; RBC, red blood cell; TBil, total bilirubin; UA, uric acid; WBC, white blood cell.

qFibrosis staging, and qFibrosis continuous values. As shown in Fig. 1A, the eGFR changes in the LF^+ group assessed by either NASH CRN staging or qFibrosis staging tended to be lower than those in the LF^- group, but was not statistically significant. In contrast, qFibrosis continuous value staging was the better method to identify eGFR changes (p = 0.043) (Fig. 1A). Therefore, it is reasonable to suggest that qFibrosis continuous values could be more sensitive to analyze the correlation between liver fibrosis progression and early renal function decline.

We stratified subjects into two groups based on their changes in eGFR and applied the above three methods (Fig. 1B). According to the NASH CRN staging, when the eGFR was elevated, there was a slightly higher rate of liver fibrosis regression (50% *vs.* 38%), whereas there was no difference in the fibrosis progression rate (23% *vs.* 22%). According to the qFibrosis staging, there was no difference in the proportion of fibrosis regression (41% *vs.* 34%), and the proportion of fibrosis progression decreased (14% *vs.* 22%) when eGFR increased. Based on the qFibrosis continuous values, the proportion of liver fibrosis regression was significantly higher (50% *vs.* 19%, p = 0.02) when eGFR increased.

Regional liver fibrosis parameters correlate with eGFR decline

Digital pathology with AI analyses was performed to investigate the temporal changes in liver fibrosis areas in five different regions. According to Spearman's nonparametric analysis, liver fibrosis characteristics in the PT/CV region and surrounding areas all negatively correlated with eGFR values in the first and second biopsies: liver fibrosis parameters increased and eGFR decreased (Fig. 2A). In addition, a higher proportion of fibrosis progression in CV and PC regions was associated with eGFR decline in these patients. Fibrosis parameters that improved over time correlated with eGFR increase (Fig. 2B and C). Table 3 shows statistical differences in 27 out of the 184 liver fibrosis parameters when we compared the eGFR increase and the eGFR decrease groups in both fibrosis regression and progression. Of these 27 hepatic fibrosis parameters, one parameter was from the PT region, 15 were from the PC region, and 11 were from the CV region. These results suggest that eGFR changes over time were more significantly correlated with liver fibrosis changes in the CV and PC region than in the PP region, zone 2, and PT region, thus suggesting that regional fibrosis progression assessment is valuable. Image examples also showed significant fibrosis regression in the CV region in the eGFR increase group, compared to the eGFR decrease group (Fig. 2D).

qFibrosis combined-index model predicts eGFR decline

The analysis of the changes in the 184 qFibrosis parameters showed that 20 hepatic fibrosis parameters significantly correlated with eGFR changes, suggesting that changes in these fibrosis parameters may specifically differentiate eGFR changes over the follow-up (the percentage of distributed collagen in the CV region (%CVDis), AUROC: 0.74, p = 0.003; the number of thin and distributed collagen fibers in the CV regions [#ThinStrCVDis], AUROC: 0.79, p = 0.000; and the length of distributed collagen fibers in the CV regions [StrLengthCVDis], AUROC: 0.74, p = 0.003) (Table S2). In addition, 14 qFibrosis parameters at baseline, including two parameters in the PT region, eight in the PC region, and four in the CV region, were able to predict changes in eGFR (Table S3). These qFibrosis parameters were higher at baseline in the eGFR-increase group than in the eGFR-decrease group, predicting an opposite trend at EOF. Five qFibrosis parameters at baseline were identified by the sequential feature selection method to calculate the qFibrosis combined index. Its diagnostic performance in predicting eGFR changes over the follow-up was evaluated using the leave-one-out cross-validation method (Fig. 3A and B) and ROC analysis (Fig. 3C). The AUROC values for the training and validation sets were 0.87 and 0.82, respectively, showing good performance in predicting eGFR decline. With a cut-off value of qFibrosis combined index = 0.52, eGFR changes could be accurately predicted using the liver fibrosis parameter at baseline.

Discussion

This explorative retrospective longitudinal study examined the relationship between liver fibrosis progression rates and eGFR decline in paired liver biopsies and serum samples from Chinese adults with MASLD over a median follow-up of 23 months. We found that as liver fibrosis progresses, eGFR declines. Our study shows for the first time that quantifying liver fibrosis with qFibrosis may provide a more accurate analysis of the relationship between the rates of liver fibrosis progression and

Table 2. Clinical and biochemical characteristics of patients with MASLD in liver fibrosis progression (QLF^+) and regression (QLF^-) groups at BL and EOF.

	QLF^+ group (n = 18)			QLF^- group (n = 23)		
	BL	EOF	*p* value	BL	EOF	*p* value
Demographics						
Age (years)	45.50 (39.75, 54.25)	46.50 (40.00, 57.00)	<0.001	39.00 (27.00, 46.00)	41.00 (30.00, 50.00)	<0.001
Male sex (%)	9 (50.00%)	9 (50.00%)	1.000	16 (69.57%)	16 (69.57%)	1.000
BMI (kg/m^2)	27.80 (23.97, 29.48)	25.92 (24.21, 28.11)	0.078	26.75 ± 4.20	25.28 ± 4.83	0.003
Diabetes, n (%)	4 (22.22%)	6 (33.33%)	0.457	4 (17.39%)	7 (30.43%)	0.300
Hypertension, n (%)	7 (38.89%)	6 (33.33%)	0.729	3 (13.04%)	4 (17.39%)	0.681
Obesity, n (%)	5 (27.78%)	4 (22.22%)	0.700	3 (13.04%)	4 (17.39%)	0.681
Waist circumference (cm)	91.00 (86.50, 99.00)	88.00 (84.50, 95.00)	0.007	92.11 ± 9.57	88.52 ± 12.66	0.094
Laboratory parameters						
WBC ($\times 10^{12}$/L)	5.84 ± 1.37	6.17 ± 1.63	0.311	5.85 (5.01, 7.37)	5.84 (4.90, 7.80)	0.858
RBC ($\times 10^{12}$/L)	4.82 ± 0.62	4.76 ± 0.62	0.312	4.84 ± 0.68	4.87 ± 0.62	0.739
Hb (g/L)	147.44 ± 16.77	145.00 ± 21.10	0.316	144.83 ± 14.90	145.74 ± 14.78	0.699
Platelet count ($\times 10^9$/L)	224.22 ± 63.23	188.00 ± 55.46	<0.001	221.61 ± 74.32	210.13 ± 67.46	0.085
TBil (μmol/L)	13.00 (10.50, 17.00)	15.50 (11.00, 42.25)	0.002	16.90 (10.60, 21.60)	21.00 (12.00, 110.00)	0.072
DBil (μmol/L)	4.18 ± 1.62	5.11 ± 2.33	0.088	4.90 (3.30, 7.00)	4.00 (3.00, 5.50)	0.016
IBil (μmol/L)	9.84 ± 4.70	11.64 ± 5.52	0.051	11.65 ± 5.77	12.89 ± 5.21	0.298
Total cholesterol (mmol/L)	5.05 ± 1.14	4.77 ± 1.23	0.119	4.85 ± 1.10	4.97 ± 1.10	0.550
Triglycerides (mmol/L)	2.44 ± 1.27	1.81 ± 0.65	0.072	2.48 ± 1.25	2.34 ± 1.19	0.674
Albumin (g/L)	43.92 ± 5.51	43.51 ± 4.73	0.721	44.93 ± 5.31	43.86 ± 3.27	0.321
ALT (U/L)	59.00 (38.50, 89.50)	41.50 (16.00, 54.50)	0.007	70.00 (45.00, 113.00)	26.00 (14.00, 68.00)	0.004
AST (U/L)	38.00 (29.75, 56.00)	28.00 (18.50, 51.25)	0.022	46.00 (33.00, 88.00)	23.00 (17.00, 42.60)	<0.001
AST/ALT ratio	0.54 (0.50, 0.94)	0.73 (0.63, 1.22)	<0.001	0.69 (0.50, 0.99)	0.90 (0.59, 1.14)	0.429
γ-Glutamyltransferase (U/L)	66.59 ± 38.62	51.76 ± 38.78	0.159	67.00 (50.00, 93.00)	30.00 (18.00, 56.00)	<0.001
BUN (mmol/L)	4.87 ± 1.13	5.19 ± 1.18	0.231	4.50 (3.70, 5.00)	5.30 (4.00, 6.30)	0.010
Scr (μmol/L)	62.63 ± 15.29	64.90 ± 16.20	0.229	68.34 ± 16.22	64.91 ± 15.01	0.047
UA (μmol/L)	363.50 (304.43, 393.75)	363.50 (287.50, 416.00)	0.286	440.15 ± 128.34	407.03 ± 133.26	0.130
eGFR ($ml/min/1.73\ m^2$)*	106.53 ± 13,71	105.28 ± 12.46	0.547	110.87 ± 14.58	114.18 ± 14.81	0.065
HDL-C (mmol/L)	0.96 (0.87, 1.10)	1.00 (0.90, 1.12)	0.224	0.92 ± 0.18	1.11 ± 0.24	<0.001
LDL-C (mmol/L)	3.10 ± 0.94	2.90 ± 0.96	0.200	3.00 ± 0.77	2.96 ± 0.78	0.793
Glucose (mmol/L)	5.80 (5.00, 8.93)	5.15 (4.75, 6.90)	0.016	5.00 (4.70, 6.40)	5.40 (4.80, 6.30)	0.485
HOMA-IR score	4.87 (3.87, 12.17)	4.24 (2.08, 6.89)	0.033	5.33 (2.76, 7.28)	3.57 (2.88, 7.41)	0.911
NFS	0.43 ± 1.54	1.05 ± 1.65	0.002	-0.03 ± 1.12	-0.00 ± 1.06	0.860
NFS category, n (%)			0.784			0.932
NFS -1.455	1 (5.56)	1 (5.56)		2 (8.70)	2 (8.70)	
-1.455≤ NFS <0.676	11 (61.11)	9 (50.0)		16 (69.57)	17 (73.91)	
NFS ≥0.676	6 (33.33)	8 (44.44)		5 (21.73)	4 (17.39)	
FIB-4 index	1.58 ± 1.53	2.15 ± 2.78	0.115	1.74 ± 1.68	1.21 ± 1.10	0.005
FIB-4 category, n (%)			0.659			0.814
FIB-4 <1.3	11 (61.11)	13 (72.22)		15 (65.22)	17 (73.92)	
1.3≤ FIB-4 <2.67	4 (22.22)	2 (11.11)		4 (17.39)	3 (13.04)	
FIB-4 ≥2.67	3 (16.67)	3 (16.67)		4 (17.39)	3 (13.04)	
CKD stage, n (%)			1.000			0.550
eGFR≥ 90 ($ml/min/1.73\ m^2$)	16 (88.89)	16 (88.89)		21 (91.30)	22 (95.65)	
60≤ eGFR< 90 ($ml/min/1.73\ m^2$)	2 (11.11)	2 (11.11)		2 (8.70)	1 (4.35)	
Liver biopsy						
Steatosis score	2.00 (1.00, 2.00)	1.00 (1.00, 1.25)	0.033	2.00 (1.00, 3.00)	1.00 (1.00, 2.00)	<0.001
Severe steatosis (%)	11 (61.11)	4 (22.22)	0.018	16 (69.57)	6 (26.09)	0.003
Ballooning score	2.00 (1.00, 2.00)	1.50 (1.00, 2.00)	0.248	2.00 (1.00, 2.00)	2.00 (1.00, 2.00)	0.710
Severe ballooning (%)	12 (66.67)	9 (50.00)	0.310	12 (52.17)	14 (60.87)	0.552

(*continued on next page*)

Table 2. (*continued*)

	QLF⁺ group (n = 18)			QLF⁻ group (n = 23)		
	BL	EOF	*p* value	BL	EOF	*p* value
Inflammation score	1.50 (1.00, 2.00)	1.00 (1.00, 1.25)	0.035	2.00 (1.00, 2.00)	1.00 (1.00, 1.00)	0.003
Severe inflammation (%)	9 (50.00)	16 (88.89)	0.011	13 (56.52)	2 (8.70)	<0.001
Fibrosis score	1.39 ± 1.33	1.67 ± 1.33	0.368	1.96 ± 1.15	1.13 ± 1.06	0.001
Severe fibrosis (%)	7 (38.89)	6 (33.33)	0.729	13 (56.52)	6 (26.09)	0.036
qFibrosis stage (qFS)	0.00 (0.00, 2.00)	2.00 (1.00, 3.00)	0.002	2.00 (2.00, 3.00)	1.00 (0.00, 2.00)	<0.001
qFibrosis continuous value (qFC)	0.83 (0.69, 1.22)	1.26 (1.04, 2.20)	<0.001	1.74 (1.18, 2.48)	0.96 (0.86, 1.20)	<0.001

Data are expressed as means ± SD, medians (P25, P75), or proportions. The paired-sample *t* test was used for comparing normally distributed continuous variables, the Wilcoxon signed-rank test for non-normally distributed variables, and the X^2 test for categorical data. *eGFR value is age- and sex-adjusted value in the second biopsy. ALT, alanine aminotransferase; AST, aspartate aminotransferase; BL, baseline; BMI, body mass index; BUN, blood urea nitrogen; CKD, chronic kidney disease; DBil, direct bilirubin; eGFR, estimated glomerular filtration rate; EOF, end of follow up; FIB-4, fibrosis-4 test; Hb, hemoglobin; HDL-C, high-density lipoprotein cholesterol; HOMA-IR, homeostatic model assessment of insulin resistance; IBil, indirect bilirubin; LDL-C, low-density lipoprotein cholesterol; NFS, non-alcoholic fatty liver disease fibrosis score; RBC, red blood cell; TBil, total bilirubin; UA, uric acid; WBC, white blood cell.

eGFR decline compared with conventional histological liver fibrosis staging systems. In addition, we performed a zonal analysis of hepatic fibrosis parameters, showing that regional liver fibrosis parameters could be more sensitive and an earlier predictor of changes in eGFR over time.

It is known that the severity of liver fibrosis is one of the strongest risk factors of long-term liver-related outcomes and all-cause mortality in people with MASLD and, therefore, an early recognition and monitoring of changes in liver fibrosis stage is essential.[2] qFibrosis provides in-depth analysis of unstained sections of liver biopsy tissue by combining the use of SHG/TPEF microscopy and AI techniques, which may reveal different collagen features, such as collagen distribution, morphology, and location.[20] Our study confirmed that qFibrosis efficiently identifies the progression and regression of liver fibrosis, as reported in animal models and patients with MASLD.[21,22] Recently, we found that qFibrosis has a clear advantage in revealing liver fibrosis regression induced by lifestyle interventions in MASLD, which is not captured by conventional histological staging.[23] qFibrosis also shows its utility for assessing subtle changes in liver fibrosis after antiviral therapy.[24]

MASLD and CKD are highly prevalent and interconnected conditions challenging global public health. It has been demonstrated that eGFR decline parallels the severity of liver fibrosis in patients with MASLD,[25] which may be explained by the overlapping pathogenesis of these two conditions. Firstly, dysregulation of lipid metabolism in MASLD or CKD patients can promote both liver fibrosis progression and kidney function decline.[26] Lipid deposition in the liver and kidneys is mainly caused by imbalances in fatty acid influx, lipid synthesis, oxidation, and export.[27] Secondly, increased oxidative stress is a common pathophysiological feature in MASLD and CKD.[28,29] Reactive oxygen species (ROS) may promote the expression of profibrotic molecules, such as transforming growth factor-β1 (TGF-β1), thus playing a significant role in developing liver and renal fibrosis. Endoplasmic reticulum (ER) stress induces proinflammatory signals from hepatocytes,[30] and prolonged ER stress can lead to increased apoptosis of renal proximal tubular cells.[31] Thirdly, insulin resistance has also been demonstrated a pathogenic factor that activates hepatic stellate cells and increases collagen matrix production, thus leading to liver fibrosis.[32] Clinical data also support the notion that insulin signaling in glomerular podocytes is important for normal renal function[33] and that insulin resistance may worsen renal function. In addition, low-grade chronic inflammation, differentially expressed genes (DEGs), and signaling pathway abnormalities are shared mechanisms underlying the development of MASLD and CKD.[32,34,35] Finally, substances, such as circulating platelet-derived growth factor-D (PDGF-D)[36] and leptin,[37] may also play a key role in hepatic and renal fibrogenesis. Our recent study also showed that serum N-terminal propeptide of collagen type 3 (PRO-C3) concentration could accurately assess liver fibrosis in MASLD-CKD patients.[38]

In the present study, we have found that eGFR changes could be distinguished earlier and more accurately based on the composite liver parameters. Changes in 20 qFibrosis parameters were found to specifically differentiate eGFR changes over the follow-up, and the qFibrosis combined index was found to predict eGFR changes, which are significant for early detection of CKD. However, the reasons these two hepatic

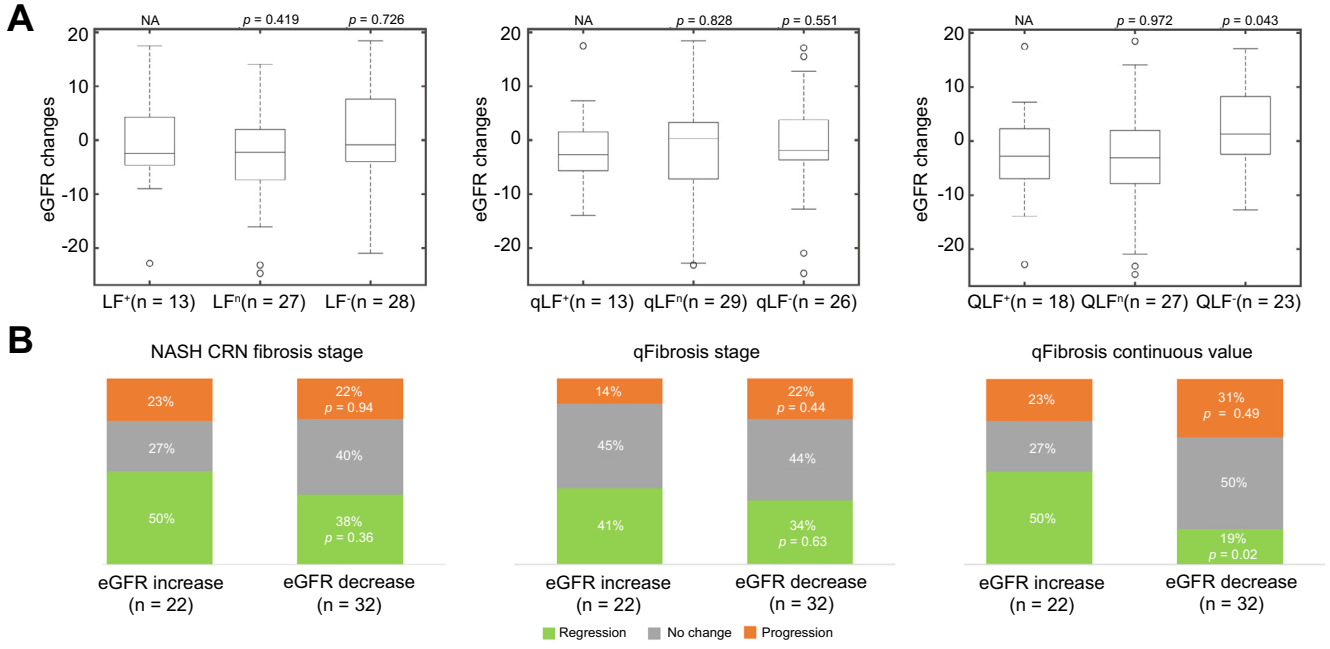

Fig. 1. Statistical differences in baseline eGFR and eGFR changes by subgroup and percentage of fibrosis changes in the eGFR increase and decrease groups by different methods. (A) Statistical differences in eGFR changes between the fibrosis no change group or regression group and the fibrosis progression group by NASH CRN score (LF^+, LF^n and LF^-), qFibrosis stage (qLF^+, qLF^n and qLF^-) and qFibrosis continuous value (QLF^+, QLF^n and QLF^-) (two-tailed Wilcoxon rank-sum test). (B) The percentage of different changes in fibrosis in patients with MASLD with increased and decreased eGFR was calculated from the NASH CRN fibrosis stage, qFibrosis stage and qFibrosis continuous value (X^2 test). CRN, Clinical Research Network; eGFR, estimated glomerular filtration rate; NASH, nonalcoholic steatohepatitis; QLF^+, liver fibrosis progression assessed by qFibrosis continuous values; QLF^-, liver fibrosis regression assessed by qFibrosis continuous values.

regions are more relevant deserve deeper investigation. Recently, Zhou *et al.*[39] reported the changes and functions of the hepatic microvasculature in three different areas during CCl_4-induced and MASH-induced liver fibrosis. They found that when the liver fibrosis progression occurred, portal vessels decreased, sinusoid capillarization increased, and central vessels increased, thus implying increased vascularity and capillarization in the CV and PC regions. These changes are also

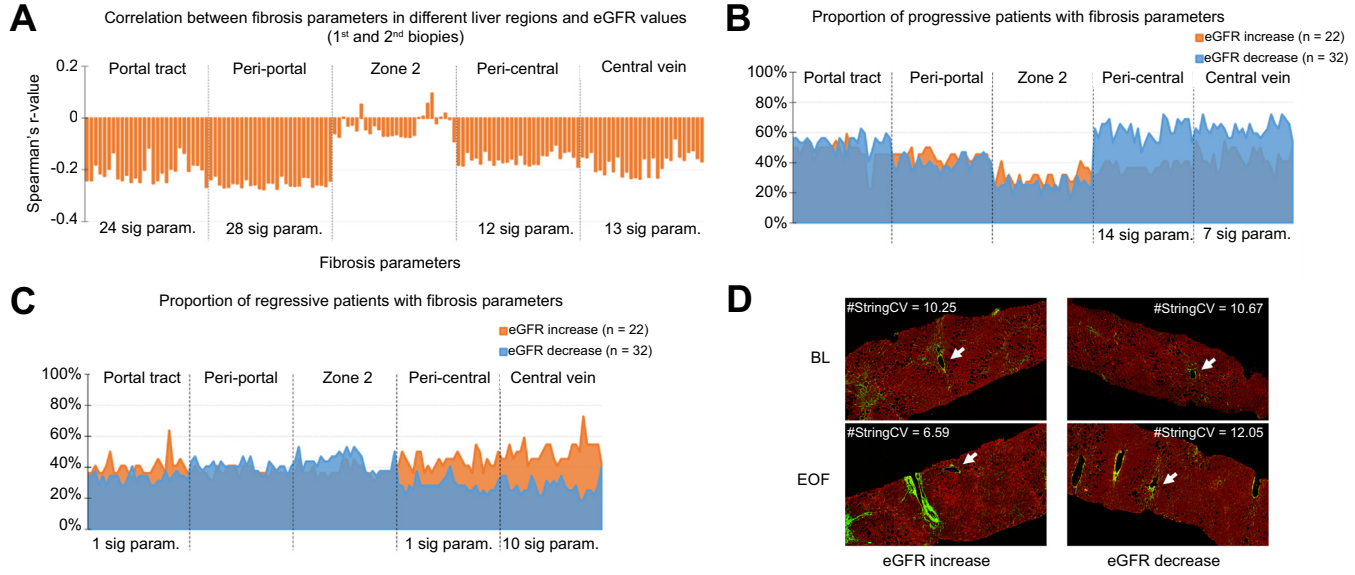

Fig. 2. Digital assessment of liver fibrosis and quantified fibrosis parameters in different liver regions demonstrated changes in fibrosis. (A) Histogram showing the correlation between liver fibrosis characteristics assessed by regional fibrosis parameters and eGFR (Spearman's rank correlation). The percentages of progressive (B) and regressive (C) patients with fibrosis parameters were calculated for the eGFR increase and decrease patients (X^2 test). (D) Examples of images showed a significant fibrosis regression in the CV region (arrows) in the eGFR increase group compared with the eGFR decrease group. CV, central vein; eGFR, estimated glomerular filtration rate.

Table 3. Twenty-seven fibrosis parameters showed significant differences in progressive or regressive liver fibrosis between the eGFR-increase and decrease groups.

		Proportion of progressive patients			Proportion of regressive patients		
Fibrosis parameter no.	Parameter regions	eGFR-increase group (%)	eGFR-decrease group (%)	*p* value	eGFR-increase group (%)	eGFR-decrease group (%)	*p* value
P1	Portal tract	23	47	0.07	64	31	0.02
P2	Pericentral	32	63	0.03	41	28	0.33
P3	Pericentral	36	66	0.03	45	22	0.07
P4	Pericentral	41	69	0.04	36	25	0.37
P5	Pericentral	32	66	0.01	36	28	0.52
P6	Pericentral	32	63	0.03	41	28	0.33
P7	Pericentral	36	66	0.03	41	28	0.33
P8	Pericentral	32	59	0.05	45	31	0.29
P9	Pericentral	41	72	0.02	41	25	0.22
P10	Pericentral	41	69	0.04	36	25	0.37
P11	Pericentral	32	59	0.05	55	28	0.05
P12	Pericentral	41	59	0.18	50	22	0.03
P13	Pericentral	41	69	0.04	36	25	0.37
P14	Pericentral	36	66	0.03	45	22	0.07
P15	Pericentral	41	69	0.04	41	25	0.22
P16	Pericentral	41	69	0.04	41	25	0.22
P17	Central vein	41	72	0.02	55	25	0.03
P18	Central vein	45	66	0.14	50	22	0.03
P19	Central vein	32	63	0.03	59	25	0.01
P20	Central vein	36	66	0.03	41	25	0.22
P21	Central vein	50	66	0.25	50	22	0.03
P22	Central vein	41	59	0.18	55	25	0.03
P23	Central vein	36	72	0.01	50	19	0.02
P24	Central vein	27	66	0.01	73	19	0.00
P25	Central vein	45	63	0.22	55	25	0.03
P26	Central vein	41	72	0.02	55	25	0.03
P27	Central vein	41	69	0.04	55	22	0.01

The X^2 test was used to estimate the statistical differences. eGFR, estimated glomerular filtration rate.

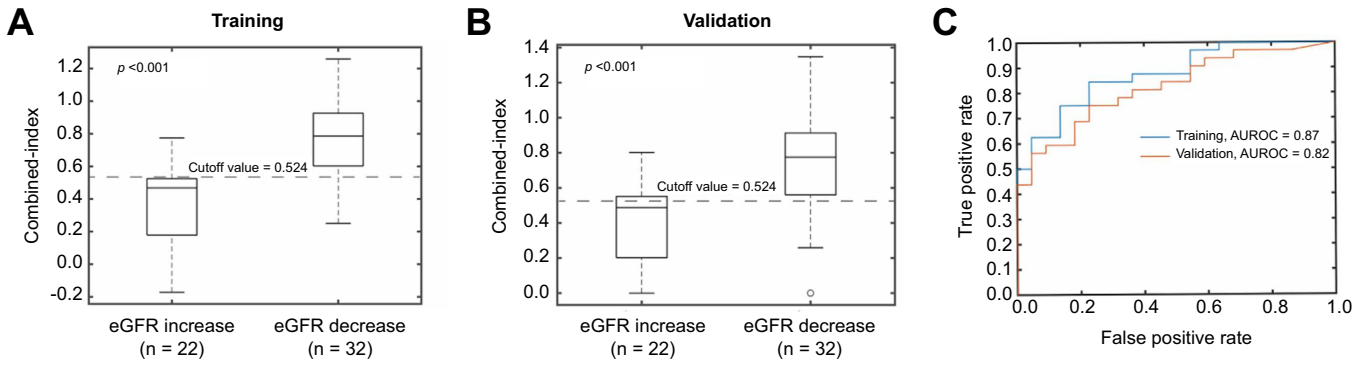

Fig. 3. qFibrosis combined index for predicting eGFR changes over the follow-up. Five parameters at baseline (%Dis, #LongStr, #ThinStrPeriPortalAgg, #LongStrCVDis and #ThinStrChickenWireAgg) were selected for the combined index. The leave-one-out cross-validation method was used. With a cut-off value of combined index = 0.52, patients with increased eGFR had lower index values than those with decreased eGFR in both training (A) and validation (B) sets (two-tailed Wilcoxon rank-sum test, p <0.001). (C) Performance of the training and validation sets in predicting eGFR changes. The area under the receiver operating characteristic curve (AUROC) analysis was used. %Dis, the percentage of distributed collagen in the tissue; #LongStr, the number of long collagen fibers in the tissue; #LongStrCVDis, the number of long and distributed collagen fibers in CV region; #ThinStrChickenWireAgg, the number of thin and aggregated collagen fibers for the chicken wire fibrosis; #ThinStrPeriPortalAgg, the number of thin and aggregated collagen fibers in peri-portal region.

associated with aberrant expression of several proangiogenic factors, such as vascular endothelial growth factors (VEGFs), fibroblast growth factors (FGFs), angiopoietins (Angs), and PDGFs,[40] which may increase liver and renal fibrogenesis. Also, because of their proximity to blood vessels, the CV and PC regions are more sensitive to aberrant expression of proinflammatory markers (*e.g.* C-reactive protein, tumor necrosis factor-alpha, and interleukin-6), lipid oxidation products (arachidonic acid oxidation products, and linoleic acid oxidation products, including hydroxy-octadecadienoic acid), indirect fibrotic biomarkers (hyaluronic acid, procollagen III amino-terminal peptide, and laminin), and microRNAs.[41,42] These factors play an important role in the progression of liver fibrosis and may also adversely affect the kidney via microcirculation, contributing to the worsening of renal function and, ultimately, to an eGFR decline.

Kidney disease poses a serious threat to human life and health, with more than 10% of the global adult population suffering from CKD.[11] Most of the previously published studies have focused on the progression and regression of liver fibrosis in patients with MASLD, but in fact, the deterioration of their kidney function is also of great significance. As mentioned earlier, the mean difference in the annual percentage change in eGFR decline in patients with MASLD compared with non-MASLD patients was approximately -1%.[17] In a clinical trial examining the progression of kidney disease, an eGFR slope reduction by 0.5 to 1.0 ml/min/1.73 m^2 per year was protective for end-stage kidney disease (multivariable-adjusted hazard ratios of 0.79 [95% CI 0.77–0.81]).[43] In addition, a nationwide population-based study demonstrated that eGFR variability of either 5% or 10% affected hard clinical outcomes, such as all-cause mortality.[44] Based on a mean follow-up of up to 23 months, we stratified eGFR changes by at least a 2% relative difference, which may seem like a small change, but hepatologists must be aware of such a decline, which might be a signal to alert clinicians to prevent and intervene in MASLD early, with the potential benefit of slowing down the deterioration of both liver and kidney disease in this patient population.

Our exploratory retrospective study has some important limitations that should be mentioned. Firstly, the sample size was small, and the follow-up time was relatively short, thus limiting the generalizability of our findings. Secondly, as our study participants were enrolled from two hospital centers in China, future research should incorporate cohorts from different countries to further validate these findings. Besides, although we adjusted eGFR levels for age, we also need to consider that ageing is a significant risk factor for all degenerative diseases. Finally, the GFR assessment using inulin is considered the reference method for measuring GFR. However, this method involves the infusion of inulin and then the measurement of blood levels after a specified period to determine the inulin clearance rate. Unfortunately, this method was unavailable in our study, so we used the widely validated creatinine-based chronic kidney disease epidemiology collaboration (CKD-EPI) equation to estimate GFR. Besides, we cannot comment on albuminuria, renal disease, or other aspects of renal tubular function.

In conclusion, the results of our exploratory retrospective longitudinal study provide potential new insights for analyzing the relationship between liver fibrosis progression rates and eGFR decline in people with biopsy-confirmed MASLD by integrating digital pathology and AI. Through digital pathology, regional liver fibrosis assessment may demonstrate specific liver lobular changes associated with early eGFR decline over time. Additional clinical research is needed to further strengthen and corroborate these findings.

Affiliations

[1]*Department of Nephrology, Jiangnan University Medical Center, Wuxi, China;* [2]*Affiliated Wuxi Clinical College of Nantong University, Wuxi, China;* [3]*Wuxi No. 2 People's Hospital, Wuxi, China;* [4]*Liver Research Center, Beijing Friendship Hospital, Beijing Key Laboratory of Translational Medicine on Liver Cirrhosis, National Clinical Research Center of Digestive Diseases, Capital Medical University, Beijing, China;* [5]*HistoIndex Pte Ltd, Singapore;* [6]*MAFLD Research Center, Department of Hepatology, the First Affiliated Hospital of Wenzhou Medical University, Wenzhou, China;* [7]*Key Laboratory of Diagnosis and Treatment for the Development of Chronic Liver Disease in Zhejiang Province, Wenzhou, China;* [8]*Institute of Hepatology, Wenzhou Medical University, Wenzhou, China;* [9]*Department of Pathology, The First Affiliated Hospital of Wenzhou Medical University, Wenzhou, China;* [10]*Southampton National Institute for Health and Care Research Biomedical Research*

Centre, University Hospital Southampton and University of Southampton, Southampton General Hospital, Southampton, UK; [11]*Department of Medicine, University of Verona, Verona, Italy;* [12]*Metabolic Diseases Research Unit, IRCCS Sacro Cuore-Don Calabria Hospital, Negrar di Valpolicella, Italy;* [13]*Hepatopancreatobiliary Center, Beijing Tsinghua Changgung Hospital, Tsinghua University, Beijing, China;* [14]*Department of Medicine and Therapeutics, Chinese University of Hong Kong, Hong Kong Special Administrative Region of China;* [15]*Stravitz-Sanyal Institute for Liver Disease and Metabolic Health, Virginia Commonwealth University School of Medicine, Richmond, VA, USA*

Abbreviations

#LongStr, the number of long collagen fibers in the tissue; #LongStrCVDis, the number of long and distributed collagen fibers in CV region; #ThinStrChickenWireAgg, the number of thin and aggregated collagen fibers for the chicken wire fibrosis; #ThinStrCVDis, the number of thin and distributed collagen fibers in the CV regions; #ThinStrPeriPortalAgg, the number of thin and aggregated collagen fibers in peri-portal region; %CVDis, the percentage of distributed collagen in the CV region; %Dis, the percentage of distributed collagen in the tissue; AI, artificial intelligence; ALT, alanine aminotransferase; Angs, angiopoietins; AST, aspartate aminotransferase; BL, baseline; BMI, body mass index; CKD, chronic kidney disease; CKD-EPI, chronic kidney disease epidemiology collaboration; CRN, Clinical Research Network; CV, central vein; CVD, cardiovascular disease; DBil, direct bilirubin; DEGs, differentially expressed genes; eGFR, estimated glomerular filtration rate; EOF, end of follow up; ER, endoplasmic reticulum; FGFs, fibroblast growth factors; FIB-4, Fibrosis-4 index; Hb, hemoglobin; HDL-C, high-density lipoprotein cholesterol; HOMA-IR, homeostatic model assessment of insulin resistance; IBil, indirect bilirubin; LDL-C, low-density lipoprotein cholesterol; MASH, metabolic dysfunction-associated steatohepatitis; MASLD, metabolic dysfunction-associated steatotic liver disease; NAFLD, nonalcoholic fatty liver disease; NASH, non-alcoholic steatohepatitis; NFS, NAFLD fibrosis score; NITs, non-invasive fibrosis tests; PC, peri-central; PDGF-D, platelet-derived growth factor-D; PP, peri-portal; PRO-C3, propeptide of collagen type 3; PT, portal tract; qFC, qFibrosis continuous; Q-FPs, quantification of fibrosis-related parameters; qFS, qFibrosis stage; QLF^-, liver fibrosis regression assessed by qFibrosis continuous values; QLF^+, liver fibrosis progression assessed by qFibrosis continuous values; RBC, red blood cell; ROS, reactive oxygen species; SHG/TPEF, second harmonic generation/two-photon excitation fluorescence; StrLengthCVDis, the length of distributed collagen fibers in the CV regions; TBil, total bilirubin; TGF-β1, transforming growth factor-β1; UA, uric acid; VEGFs, vascular endothelial growth factors; WBC, white blood cell.

Financial support

This work was supported by grants from the National Key R&D Program of China (2023YFA1800801), Noncommunicable Chronic Diseases-National Science and Technology Major Project (2023ZD0508700), National Natural Science Foundation of China (82370577, 82070588, 82000690). D-S is supported in part by grants from the Top Talent Support Program for young and middle-aged people of Wuxi Health Committee (BJ2023023), Taihu Light Scientific and Technology research project (Y2032011) and supported by China Postdoctoral Science Foundation (2023M732681). CDB is supported in part by the Southampton NIHR Biomedical Research Center (NIHR 203319), UK. GT is supported in part by grants from the University School of Medicine of Verona, Verona, Italy.

Conflicts of interest

The authors have no conflicts of interest to declare.

Please refer to the accompanying ICMJE disclosure forms for further details.

Authors' contributions

Designed the study: D-QS, M-HZ. Contributed to data collection and resource acquisition: H-YY, X-FT, Y-YL, S-DC, X-ZJ, X-DW, HY. Drafted the manuscript: J-QS. Worked on visualization of data: Y-YR, X-LW. Contributed to revising and proofreading the manuscript: LW, VW-SW, DT, AJS, CDB, GT.

Data availability statement

The datasets generated and analyzed during the current study are not publicly available because of other unpublished data but are available from the corresponding author on reasonable request.

Acknowledgements

The investigators are grateful to all participants for their cooperation in the study.

Supplementary data

Supplementary data to this article can be found online at https://doi.org/10.1016/j.jhepr.2025.101358.

References

Author names in bold designate shared co-first authorship

[1] Rinella ME, Lazarus JV, Ratziu V, et al. A multisociety Delphi consensus statement on new fatty liver disease nomenclature. J Hepatol 2023;79:1542–1556.
[2] Miao L, Targher G, Byrne CD, et al. Current status and future trends of the global burden of MASLD. Trends Endocrinol Metab 2024;35:697–707.
[3] Schuster S, Cabrera D, Arrese M, et al. Triggering and resolution of inflammation in NASH. Nat Rev Gastroenterol Hepatol 2018;15:349–364.
[4] **Targher G**, **Byrne CD**, **Tilg H**. MASLD: a systemic metabolic disorder with cardiovascular and malignant complications. Gut 2024;73:691–702.
[5] Ekstedt M, Hagström H, Nasr H, et al. Fibrosis stage is the strongest predictor for disease-specific mortality in NAFLD after up to 33 years of follow-up. Hepatology 2015;61:1547–1554.
[6] European Association for the Study of the Liver. EASL-EASD-EASO Clinical Practice Guidelines on the management of metabolic dysfunction-associated steatotic liver disease (MASLD). J Hepatol 2024;81:492–542.
[7] **Xu S**, **Wang Y**, Tai DCS, et al. qFibrosis: a fully-quantitative innovative method incorporating histological features to facilitate accurate fibrosis scoring in animal model and chronic hepatitis B patients. J Hepatol 2014;61:260–269.
[8] Liu F, Goh GB, Tiniakos D, et al. qFIBS: an automated technique for quantitative evaluation of fibrosis, inflammation, ballooning, and steatosis in patients with nonalcoholic steatohepatitis. Hepatology 2020;71:1953–1966.
[9] Wang Y, Vincent R, Yang J, et al. Dual-photon microscopy-based quantitation of fibrosis-related parameters (q-FP) to model disease progression in steatohepatitis. Hepatology 2017;65:1891–1903.
[10] Liu F, Zhao JM, Rao HY, et al. Second harmonic generation reveals subtle fibrosis differences in adult and pediatric nonalcoholic fatty liver disease. Am J Clin Pathol 2017;148:502–512.
[11] Kalantar-Zadeh K, Jafar TH, Nitsch D, et al. Chronic kidney disease. Lancet 2021;398:786–802.
[12] Chan KE, Ong EYH, Chung CH, et al. Longitudinal outcomes associated with metabolic dysfunction-associated steatotic liver disease: a meta-analysis of 129 studies. Clin Gastroenterol Hepatol 2024;22. 488–98.e14.
[13] Younossi ZM, Kalligeros M, Henry L. Epidemiology of metabolic dysfunction-associated steatotic liver disease. Clin Mol Hepatol 2025;31(Suppl):S32–S50.
[14] Sandireddy R, Sakthivel S, Gupta P, et al. Systemic impacts of metabolic dysfunction-associated steatotic liver disease (MASLD) and metabolic dysfunction-associated steatohepatitis (MASH) on heart, muscle, and kidney related diseases. Front Cell Dev Biol 2024;12:1433857.
[15] Sun DQ, Jin Y, Wang TY, et al. MAFLD and risk of CKD. Metabolism 2021;115:154433.
[16] Wang TY, Wang RF, Bu ZY, et al. Association of metabolic dysfunction-associated fatty liver disease with kidney disease. Nat Rev Nephrol 2022;18:259–268.
[17] Jang HR, Kang D, Sinn DH, et al. Nonalcoholic fatty liver disease accelerates kidney function decline in patients with chronic kidney disease: a cohort study. Sci Rep 2018;8:4718.
[18] Kleiner DE, Brunt EM, Van Natta M, et al. Design and validation of a histological scoring system for nonalcoholic fatty liver disease. Hepatology 2005;41:1313–1321.
[19] Brunt EM, Janney CG, Di Bisceglie AM, et al. Nonalcoholic steatohepatitis: a proposal for grading and staging the histological lesions. Am J Gastroenterol 1999;94:2467–2474.
[20] Gailhouste L, Le Grand Y, Odin C, et al. Fibrillar collagen scoring by second harmonic microscopy: a new tool in the assessment of liver fibrosis. J Hepatol 2010;52:398–406.
[21] Ng N, Tai D, Ren Y, et al. Second-harmonic generated quantifiable fibrosis parameters provide signatures for disease progression and regression in nonalcoholic fatty liver disease. Clin Pathol 2023;16:2632010x231162317.
[22] Wang XX, Jin R, Li XH, et al. Collagen co-localized with macrovesicular steatosis better differentiates fibrosis progression in non-alcoholic fatty liver disease mouse models. Front Med (Lausanne) 2023;10:1172058.

[23] Yuan HY, Tong XF, Ren YY, et al. AI-based digital pathology provides newer insights into lifestyle intervention-induced fibrosis regression in MASLD: an exploratory study. Liver Int 2024;44:2572–2582.
[24] Sun Y, Zhou J, Wu X, et al. Quantitative assessment of liver fibrosis (qFibrosis) reveals precise outcomes in Ishak "stable" patients on anti-HBV therapy. Sci Rep 2018;8:2989.
[25] Targher G, Bertolini L, Rodella S, et al. Relationship between kidney function and liver histology in subjects with nonalcoholic steatohepatitis. Clin J Am Soc Nephrol 2010;5:2166–2171.
[26] Mitrofanova A, Merscher S, Fornoni A. Kidney lipid dysmetabolism and lipid droplet accumulation in chronic kidney disease. Nat Rev Nephrol 2023;19:629–645.
[27] Yang M, Geng CA, Liu X, et al. Lipid disorders in NAFLD and chronic kidney disease. Biomedicines 2021;9:1405.
[28] Gyurászová M, Gurecká R, Bábíčková J, et al. Oxidative stress in the pathophysiology of kidney disease: implications for noninvasive monitoring and identification of biomarkers. Oxid Med Cell Longev 2020;2020:5478708.
[29] Masarone M, Rosato V, Dallio M, et al. Role of oxidative stress in pathophysiology of nonalcoholic fatty liver disease. Oxid Med Cell Longev 2018;2018:9547613.
[30] Baral A, Park PH. Leptin induces apoptotic and pyroptotic cell death via NLRP3 inflammasome activation in rat hepatocytes. Int J Mol Sci 2021;22:12589.
[31] Lhoták S, Sood S, Brimble E, et al. ER stress contributes to renal proximal tubule injury by increasing SREBP-2-mediated lipid accumulation and apoptotic cell death. Am J Physiol Ren Physiol 2012;303:F266–F278.
[32] Byrne CD, Targher G. NAFLD as a driver of chronic kidney disease. J Hepatol 2020;72:785–801.
[33] Thomas SS, Zhang L, Mitch WE. Molecular mechanisms of insulin resistance in chronic kidney disease. Kidney Int 2015;88:1233–1239.
[34] Loomba R, Friedman SL, Shulman GI. Mechanisms and disease consequences of nonalcoholic fatty liver disease. Cell 2021;184:2537-–25364.
[35] Li X, Bhattacharya D, Yuan Y, et al. Chronic kidney disease in a murine model of non-alcoholic steatohepatitis (NASH). Kidney Int 2024;105:540–561.
[36] Borkham-Kamphorst E, Alexi P, Tihaa L, et al. Platelet-derived growth factor-D modulates extracellular matrix homeostasis and remodeling through TIMP-1 induction and attenuation of MMP-2 and MMP-9 gelatinase activities. Biochem Biophys Res Commun 2015;457:307–313.
[37] Alix PM, Guebre-Egziabher F, Soulage CO. Leptin as an uremic toxin: deleterious role of leptin in chronic kidney disease. Biochimie 2014;105:12–21.
[38] Tang LJ, Sun DQ, Song SJ, et al. Serum PRO-C3 is useful for risk prediction and fibrosis assessment in MAFLD with chronic kidney disease in an Asian cohort. Liver Int 2024;44:1129–1141.
[39] Lin Y, Dong MQ, Liu ZM, et al. A strategy of vascular-targeted therapy for liver fibrosis. Hepatology 2022;76:660–675.
[40] Coulon S, Heindryckx F, Geerts A, et al. Angiogenesis in chronic liver disease and its complications. Liver Int 2011;31:146–162.
[41] Di Mauro S, Scamporrino A, Filippello A, et al. Clinical and molecular biomarkers for diagnosis and staging of NAFLD. Int J Mol Sci 2021;22:11905.
[42] Gjorgjieva M, Sobolewski C, Dolicka D, et al. miRNAs and NAFLD: from pathophysiology to therapy. Gut 2019;68:2065–2079.
[43] Levey AS, Gansevoort RT, Coresh J, et al. Change in albuminuria and GFR as end points for clinical trials in early stages of CKD: a scientific workshop sponsored by the National Kidney Foundation in collaboration with the US Food and Drug Administration and European Medicines Agency. Am J Kidney Dis 2020;75:84–104.
[44] Lee S, Park S, Kim Y, et al. Impact of variability in estimated glomerular filtration rate on major clinical outcomes: a nationwide population-based study. PLoS One 2020;15:e0244156.

Keywords: Metabolic dysfunction-associated steatotic liver disease; Regional liver fibrosis; Kidney function; Digital pathology; Metabolic dysfunction-associated fatty liver disease.

Received 16 October 2024; received in revised form 5 February 2025; accepted 10 February 2025; Available online 12 February 2025